International Journal of Architecture and Urbanism Vol. 10, No. 02 (2026) 165 – 181

talenta PUBLISHER

International Journal of Architecture and Urbanism

Journal homepage: https://talenta.usu.ac.id/ijau

Research On The Classification of Calculation Schema of The Column-Foundation Connections

Ju Su Haeng*[1], Jong Mun Il[1], Jun TokGo[1]

[1]*Pyongyang University of Architecture, Pyongyang DPR Korea*

*Corresponding Author: dawei_0660@163.com

ARTICLE INFO

Article history:
Received 15 November 2024
Revised 14 November 2025
Accepted 30 April 2026
Available online 30 August 2026

E-ISSN: 2622-1640
P-ISSN: 2622-0008

How to cite:
Haeng, J. S., Il, J. M. Research On The Classification of Calculation Schema of The Column-Foundation Connections. International Journal of Architecture and Urbanism. 2026. 10(2):165-181.

http://doi.org 10.32734/ijau.v10i2.18881

ABSTRACT

Exposed steel column bases are commonly idealized as either pinned or fixed, although their actual response is governed by finite rotational stiffness arising from base-plate bending, anchor-bolt elongation, contact separation, and concrete bearing. This study investigates the deformation behavior and classification of exposed column–foundation connections through three-dimensional finite-element analysis in Abaqus. Thirteen connection models were developed by varying the number and location of anchor bolts and the arrangement of stiffeners. The models incorporated a steel H-section column, steel base plate, concrete foundation, anchor bolts, nonlinear contact, and combined horizontal and vertical loading. Connection rotation was evaluated from relative vertical displacements at selected points on the base plate, and rotational stiffness was related to anchor-bolt axial stiffness, effective lever arms, and plate flexibility. The results show that nominally pinned bases can transfer bending moment, while nominally rigid bases may undergo appreciable rotation. External anchor bolts and properly oriented stiffeners generally reduced deformation, although excessive plate projection increased local flexibility. A normalized stiffness ratio, (k/(EI/L)), was proposed to classify connection behavior. Ratios below 2 indicate hinged behavior, ratios between 2 and 24 indicate semi-rigid behavior, and ratios above 24 indicate rigid behavior. The framework links local connection mechanics with global column stability.

Keywords: anchor bolts, exposed column base, finite-element analysis, rotational stiffness, semi-rigid connection

1. Introduction

The connection between a steel column and its concrete foundation is a critical component of a steel structural system because it transfers axial force, shear force, and bending moment from the superstructure to the foundation. The behavior of this connection influences the distribution of internal forces, lateral deformation, buckling resistance, and overall structural stability. In conventional structural analysis, column–foundation connections are frequently idealized as either perfectly hinged or perfectly rigid. A hinged connection is assumed to permit unrestricted rotation without transferring bending moment, whereas a rigid connection is assumed to prevent rotation completely. In practice, however, exposed steel column bases generally possess finite rotational stiffness and therefore behave between these two idealized conditions. Column bases may be classified according to their structural idealization and constructional form. Based on the calculation schema, they are commonly represented as hinged, semi-rigid, or rigid connections. Based on their construction, they may be categorized as exposed or embedded column bases. An exposed column base generally consists of a steel column, a base plate, anchor bolts, grout, and a reinforced-concrete foundation. This system is frequently used in industrial buildings and other lightweight steel structures because the concrete foundation can be constructed before the steel frame is erected, thereby simplifying installation and reducing construction time. Exposed bases also provide relatively easy access for inspection, adjustment, and maintenance.

Despite these practical advantages, the actual behavior of an exposed column base is more complex than its nominal designation. A connection detailed as a hinge can still resist bending moment through the elongation of anchor bolts, deformation of the base plate, friction, and bearing against the concrete foundation. Conversely, a connection detailed as rigid can experience significant rotation because of local plate bending, anchor-bolt deformation, contact separation, grout deformation, and concrete compression. Consequently, an inappropriate boundary-condition assumption may result in inaccurate predictions of column effective length, critical buckling load, structural displacement, and force distribution. Ermopoulos and Stamatopoulos developed a mathematical model for column-base plate connections and demonstrated that their response depends on the mechanical interaction among the base plate, anchor bolts, and concrete support [1]. Their work indicates that column-base behavior cannot be represented adequately by considering only the nominal connection arrangement. The stiffness and resistance of the connection must instead be derived from the deformation and force-transfer mechanisms of its constituent components.

Jaspart and Vandegans applied the component method to column bases by representing a connection as an assembly of individual tension, compression, and bending components [2]. Under this approach, the global moment–rotation response is determined from the stiffness, resistance, and deformation capacity of the individual components. The component method provides a rational framework for explaining why changes in anchor-bolt arrangement, plate geometry, concrete bearing, and stiffener configuration can produce different rotational responses, even when the connections are assigned the same nominal classification.

Experimental investigations by Hon and Melchers showed that the behavior of steel column bases is influenced by parameters such as base-plate thickness, anchor-bolt dimensions, and connection geometry [3]. Their observations support the conclusion that exposed column bases exhibit measurable rotational flexibility and that neither the ideal hinge nor the ideal fixed condition can fully represent all practical configurations. Experimental evidence is therefore essential for identifying the governing deformation modes and evaluating the validity of analytical or numerical models. Eurocode 3 provides general requirements for the analysis and design of steel structures, including the treatment of structural stability, member stiffness, resistance, and the assumptions used in global analysis [4]. These provisions emphasize that the structural model should represent the expected behavior of the actual system with sufficient accuracy. Accordingly, the classification of a column base should consider its rotational stiffness relative to the stiffness of the connected column rather than relying exclusively on constructional details or nominal connection labels.

Previous analytical, component-based, and experimental studies have established the principal mechanisms governing column-base behavior [1][2][3]. Nevertheless, a practical criterion is still required to determine when an exposed column base can be represented as hinged, semi-rigid, or rigid in a structural calculation model. The absolute value of the connection rotational stiffness is not sufficient for this purpose because the structural effect of a given connection stiffness also depends on the flexural rigidity and length of the connected column. The same column base may behave approximately as a rigid support for a flexible column but as a semi-rigid or flexible support for a shorter and stiffer column. This study therefore investigates the deformation behavior and rotational stiffness of exposed steel column bases with different anchor-bolt and stiffener arrangements. Thirteen three-dimensional finite-element models are analyzed using Abaqus. The effects of anchor-bolt number, anchor-bolt position, plate deformation, and stiffener arrangement are examined. A simplified expression for estimating the rotational stiffness of an exposed column base is then considered based on the deformation of its principal components. Finally, the calculated connection stiffness is normalized by the column stiffness per unit length, and the resulting ratio is evaluated against column buckling loads to establish quantitative limits for hinged, semi-rigid, and rigid connection idealizations.

The main contribution of this study is the proposed classification of exposed column-foundation connections using the relative stiffness ratio k/i_c, where k is the rotational stiffness of the column base and $i_c = EI / L$ is the stiffness of the connected column per unit length. The proposed approach links local connection behavior to the global response of the column and provides a more rational basis for selecting the calculation schema than classification based solely on the position of the anchor bolts.

2. Method

This research employed three-dimensional finite-element analysis and theoretical stiffness evaluation to investigate the behavior of exposed steel column–foundation connections. The methodological framework combined the force-transfer mechanisms identified in the mathematical model proposed by Ermopoulos and Stamatopoulos [1], the component-based interpretation presented by Jaspart and Vandegans [2], and the deformation mechanisms observed experimentally by Hon and Melchers [3]. The global analysis and column-stability assessment were formulated consistently with the general structural-analysis principles of Eurocode 3 [4].

The investigation was conducted in three principal stages. First, the deformation behavior of thirteen exposed column-base configurations was analyzed under combined vertical and horizontal loading. Second, the rotational stiffness of each connection was evaluated from the applied bending moment and the calculated local rotation of the base plate. Third, column buckling analyses were performed to determine the relationship between the rotational stiffness of the column base and the flexural stiffness of the connected column. This relationship was used to establish the proposed limits for hinged, semi-rigid, and rigid calculation schemas.

An exposed steel column base was defined as a connection in which the steel column was welded to a base plate and connected to a reinforced-concrete foundation by anchor bolts embedded in the concrete. Grout was assumed to be provided beneath the base plate to level the foundation surface and ensure effective contact between the plate and the concrete support. The typical column-base configurations considered in the study are presented in Figure 1. Figure 1(a) represents an idealized hinge incorporating a roller mechanism. Figure 1(b) represents a nominally hinged base with anchor bolts located near the column center. Figure 1(c) represents a nominally rigid base with the anchor bolts positioned farther from the column center. Figure 1(d) represents a strengthened connection incorporating stiffeners and wing plates to increase rotational stiffness and bearing resistance.

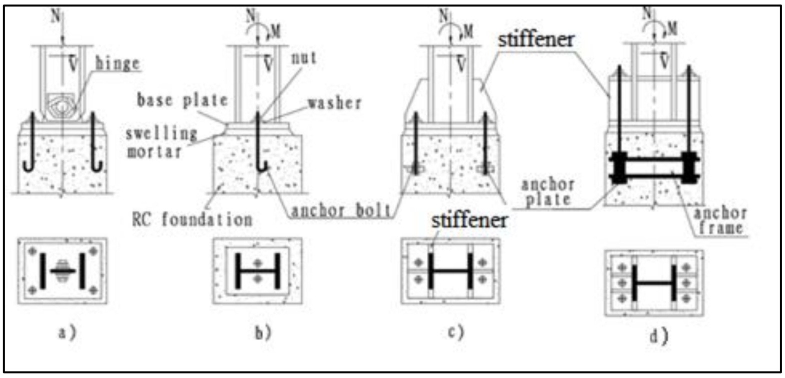

Figure 1. Steel exposed column base

The anchor-bolt layouts investigated in the finite-element analysis are presented in Figure 2. Thirteen models were developed to evaluate the effects of bolt number, bolt position, and stiffener arrangement. Models 1–4 contained anchor bolts located inside the column flanges and were initially regarded as nominally hinged bases. Models 5–11 contained anchor bolts outside the column flanges and were initially regarded as nominally rigid bases. Model 12 combined two internal anchor bolts and two external anchor bolts. Model 13 combined four internal bolts, four external bolts, and four stiffeners. This model matrix allowed the effects of individual detailing parameters to be assessed while maintaining the same principal column, plate, foundation, and anchor-bolt dimensions.

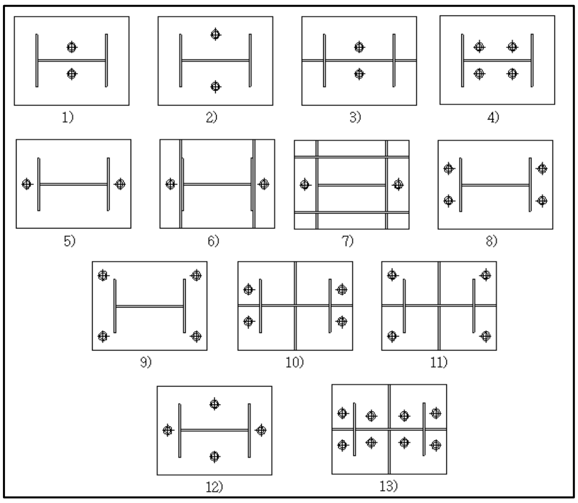

Figure 2. arrangement method of anchor bolts in the steel exposed column base

The steel column had an H-shaped section of H440 × 300 × 10 × 16 mm. The base plate measured 900 × 700 mm and had a thickness of 36 mm. The reinforced-concrete foundation had a plan dimension of 1200 × 950 mm and a depth of 1500 mm. The anchor bolts had a nominal diameter of 36 mm and an embedded length of 1000 mm. The column and base plate were assigned the specified grade-235 steel properties, while the concrete foundation was modeled using the specified C20 concrete properties. The anchor bolts were assigned their corresponding elastic and strength properties. For complete reproducibility, the final manuscript should report the numerical values of Young's modulus, Poisson's ratio, yield strength, ultimate strength, and concrete compressive strength used in the Abaqus material definitions.

The mechanical representation of the connection followed the component concept described in [2]. The tension region consisted primarily of the anchor bolts and the adjacent projecting base plate, while the compression region consisted of the base plate bearing against the concrete foundation. The stiffeners were modeled as additional components that increased the out-of-plane rigidity of the base plate and improved the transfer of column-flange forces. This representation was also consistent with the experimental mechanisms reported in [3], including plate bending, bolt elongation, and localized concrete bearing.

All components were modeled using the Abaqus C3D8R element, an eight-node linear brick element with reduced integration. The mesh configuration is illustrated in Figure 3. Approximately 3000 elements were used for the steel column, 4000 elements for the concrete foundation, and 2000 elements for the base plate. Approximately 500 additional elements were assigned to the anchor bolts, nuts, and stiffeners. The resulting finite-element models contained approximately 9000–10,000 elements each. The mesh was refined in the vicinity of the base plate, anchor bolts, column flanges, and concrete contact region because high stress and deformation gradients were expected in these locations.

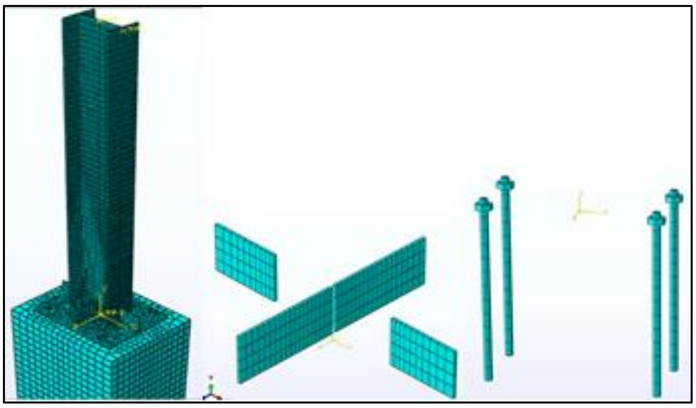

Figure 3. Mesh of the elements for the column base

Tie constraints were used to represent connections assumed to have no relative movement, including the welded connection between the steel column and base plate and the connection between each anchor bolt and its nut. Surface-to-surface contact was used between the base plate and concrete foundation and between the nuts, anchor bolts, and base plate where contact interaction was required. A friction coefficient of 0.40 was assigned to the base plate–foundation interface, while a coefficient of 0.15 was assigned to the relevant steel-to-steel contact interfaces. The embedded-region constraint was used to connect the embedded portions of the anchor bolts to the concrete foundation.

The use of nonlinear contact was necessary because the base plate could separate from the foundation on the tension side while remaining in compression contact on the opposite side. This opening and closing mechanism influences the location of the compression resultant and the tension forces developed in the anchor bolts. The mathematical treatment of the connection therefore considered both the tensile response of the anchor bolts and the bearing response of the base plate and foundation, consistent with the modeling principles discussed in [1] and [2].

A horizontal load of $P_h = 800$ kN and a vertical load of $P_v = 500$ kN were applied at the top of the steel column. The horizontal load generated bending moment at the column base, while the vertical load represented the axial force transferred from the steel column to the foundation. The loading generated tension in the anchor bolts on one side of the connection and compression beneath the base plate on the opposite side. The bottom and appropriate external surfaces of the concrete foundation were restrained to prevent rigid-body motion and represent the support provided by the surrounding foundation system.

The local rotation of the column base was evaluated from the vertical displacements of two points on the upper surface of the base plate, as illustrated in Figure 4. The first monitoring point was positioned near the center of the base plate, while the second was positioned at the centerline of the tension-side column flange. The rotational angle was calculated as

$$\theta = \frac{\Delta_i - \Delta_j}{y_i - y_j}, \tag{1}$$

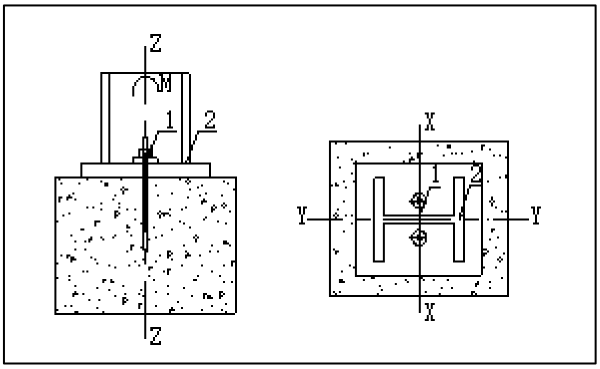

Figure 4. Points to consider the deformation of the base plate

Where θ is the angular deformation of the base plate in radians, Δi and Δj are the vertical displacements of the selected points, and and are their corresponding coordinates in the direction of bending. The calculated value represents the connection rotation associated with the relative vertical deformation of the two monitoring points.

The rotational stiffness of the column base was determined from the relationship between the applied bending moment and the calculated connection rotation. Its theoretical formulation was based on the axial stiffness of the tension-side anchor bolts and the effective distance between the tension and compression resultants. The parameters included the sectional area of one tensioned anchor bolt, the elastic modulus and effective embedded length of the bolt, the number of active tension-side bolts, the distance from the column-base center to the tension-bolt group, the distance from the column-base center to the compression zone, and a reduction factor representing base-plate flexibility. The reduction factor was used to distinguish stiffened and unstiffened configurations because part of the total connection rotation resulted from base-plate deformation rather than anchor-bolt elongation alone.

This stiffness formulation reflects the component-based principle that the global rotation of a connection results from the combined deformation of its constituent components [2]. The anchor bolts were treated as axial tension components, while the base plate and concrete contact zone provided the corresponding compression and bending components. The experimental findings in [3] were used as the mechanical basis for considering bolt size and plate deformation as principal variables. The formulation also followed the analytical concept in [1], in which connection stiffness is derived from the equilibrium and compatibility of the tension and compression regions.

The final stage of the methodology assessed the effect of connection stiffness on column buckling. Ten steel-column configurations with different section dimensions and lengths were selected, as listed in Table 1. Their stiffness per unit length was calculated as

$$i_c = \frac{EI}{L}, \tag{2}$$

Table 1. Section size and length of the column used in buckling analysis

No	Dimension of the steel column section				Length of the column(m)
	h_w (mm)	b_w(mm)	h_f(mm)	b_f(mm)	
1	408	10	16	300	21.6
2	372	10	14	270	18
3	356	8	12	250	14.4
4	340	8	10	240	10.8
5	418	12	16	300	21.6
6	372	10	14	270	21.6
7	356	8	12	250	7.2
8	340	8	10	240	18
9	418	12	16	300	18
10	372	10	14	270	14.4

Where E is the Young's modulus of the steel column, I is the second moment of area about the relevant buckling axis, and L is the column length. This parameter was selected because the structural significance of the base rotational stiffness depends on the relative flexibility of the connected column.

The normalized connection-stiffness parameter was defined as

$$\rho = \frac{k}{i_c}, \tag{3}$$

Where k is the rotational stiffness of the column base and i_c is the stiffness of the column per unit length. Although the original table heading should be checked, the numerical values reported in Tables 2 and 3 correspond to k/i_c, not i_c/k. The dimensionless ratio was subsequently used as the principal parameter for classifying the column–foundation connection.

Table 2. Comparison analysis in the column base which was considered like hinge column base

No	Stiffness per unit length i_c *(kN·m)*	Rotational stiffness of the column base calculated by Abaqus *k (kN·m)*	i_c/k	Buckling load calculated by Abaqus $N_{cr}(kN)$	Euler critical load (hinge-hinge) $N_{cr}(kN)$	error (%)
a1	4747.02	8609.00	1.81	2290.00	2166.84	5.68
a2	4428.68	8178.55	1.85	2567.50	2425.83	5.84
a3	4298.45	7748.10	1.80	3109.41	2943.12	5.65
a4	4587.17	7403.74	1.61	4390.85	4187.74	4.85
a5	4906.82	9986.44	2.04	2388.50	2239.78	6.64
a6	3690.57	8178.55	2.22	1809.44	1684.61	7.41
a7	8596.89	7748.10	0.90	11558.23	11772.49	1.82
a8	2752.30	7403.74	2.69	1649.60	1507.6	9.42
a9	5888.24	9986.44	1.70	3393.03	3225.32	5.20
a10	5535.93	8178.55	1.48	3952.27	3790.42	4.27
b1	4747.02	25314.2	5.33	2613.97	2166.84	20.6
b2	4428.68	24048.49	5.43	2936.74	2425.83	21.1
b3	4298.45	22782.78	5.30	3546.72	2943.12	20.5
b4	4587.17	21770.212	4.75	4947.97	4187.74	18.2
b5	4906.82	29364.472	5.98	2764.24	2239.78	23.4
b6	3690.57	24048.49	6.52	2117.13	1684.61	25.7
b7	8596.89	22782.78	2.65	12861.37	11772.49	9.25
b8	2752.30	21770.212	7.91	1983.93	1507.59	31.6
b9	5888.24	29364.472	4.99	3843.86	3225.32	19.2
b10	5535.93	24048.49	4.34	4413.81	3790.42	16.4
c1	4747.02	50628.40	10.7	3108.60	2166.84	43.5
c2	4428.68	48096.98	10.9	3496.69	2425.83	44.1
c3	4298.45	45565.56	10.6	4209.83	2943.12	43
c4	4587.17	43540.42	9.5	5792.81	4187.74	38.3
c5	4906.82	58728.94	12.0	3334.03	2239.78	48.9
c6	3690.57	48096.98	13.0	2583.77	1684.61	53.4
c7	8596.89	45565.56	5.3	14187.44	11772.49	20.5
c8	2752.30	43540.42	15.8	2490.85	1507.59	65.2
c9	5888.24	58728.94	10.0	4527.60	3225.32	40.4
c10	5535.93	48096.98	8.7	5113.74	3790.42	34.9
a11	2607.44	7403.74	2.8	1489.1	1353.07	10.1
b11	11462.53	22782.78	2.0	22276.3	20928.87	6.4
c11	17329.62	48096.98	2.8	40957.3	37144.16	10.3

Table 3. Comparison analysis in the column base which was considered like rigid column base

No	Stiffness per unit length i_c *(kN·m)*	Rotational stiffness of the column base calculated by Abaqus *k (kN·m)*	i_c/k	Buckling load calculated by Abaqus $N_{cr}(kN)$	Euler critical load (hinge-hinge) $N_{cr}(kN)$	error (%)
c1	4747.02	108986.00	22.96	515.3	541.71	4.88
c2	4428.68	103536.70	23.38	586.70	606.46	3.26
c3	4298.45	101356.98	23.58	718.16	735.78	2.40
c4	4587.17	96997.54	21.15	912.65	1046.94	12.83
c5	4906.82	119884.60	24.43	552.91	559.95	1.26

No	Stiffness per unit length i_c (kN·m)	Rotational stiffness of the column base calculated by Abaqus k (kN·m)	i_c/k	Buckling load calculated by Abaqus N_{cr}(kN)	Euler critical load (hinge-hinge) N_{cr}(kN)	error (%)
c6	3690.57	103536.70	28.05	417.74	421.152	0.81
c7	8596.89	101356.98	11.79	1385.87	2943.12	52.91
c8	2752.30	96997.54	35.24	375.2	376.9	0.45
c9	5888.24	119884.60	20.36	675.77	806.33	16.19
c10	5535.93	103536.70	18.70	726.88	947.61	23.29
b1	4747.02	54493	11.48	247.88	541.71	54.2
b2	4428.68	51768.35	11.69	282.96	606.46	53.3
b3	4298.45	50678.49	11.79	346.47	735.78	52.91
b4	4587.17	48498.77	10.57	438.38	1046.94	58.12
b5	4906.82	59942.3	12.22	273.89	559.95	51.08
b6	3690.57	51768.35	14.03	238.69	421.15	43.32
b7	8596.89	50678.49	5.89	642.49	2943.12	78.17
b8	2752.30	48498.77	17.62	271.64	376.90	27.92
b9	5888.24	59942.3	10.18	324.07	806.33	59.81
b10	5535.93	51768.35	9.35	347.20	947.61	63.36
a1	4747.02	27246.5	5.74	114.65	541.71	78.83
a2	4428.68	25884.2	5.84	131.08	606.46	78.3
a3	4298.45	25339.2	5.89	160.62	735.78	78.17
a4	4587.17	24249.4	5.29	201.25	1046.94	80.77
a5	4906.82	29971.2	6.11	127.35	559.95	77.25
a6	3690.57	25884.2	7.01	112.12	421.15	73.37
a7	8596.89	25339.2	2.95	270.81	2943.12	90.79
a8	2752.30	24249.4	8.81	129.36	376.90	65.67
a9	5888.24	29971.2	5.09	148.21	806.33	81.61
a10	5535.93	25884.2	4.68	157.36	947.61	83.39

For the nominally hinged configurations shown in Figure 5, the critical buckling loads obtained from Abaqus were compared with the Euler critical loads calculated for the corresponding ideal hinged condition. The relative difference was calculated as

$$e = \left| \frac{N_{\mathrm{cr,FE}} - N_{\mathrm{cr,Euler}}}{N_{\mathrm{cr,Euler}}} \right| \times 100\%, \tag{4}$$

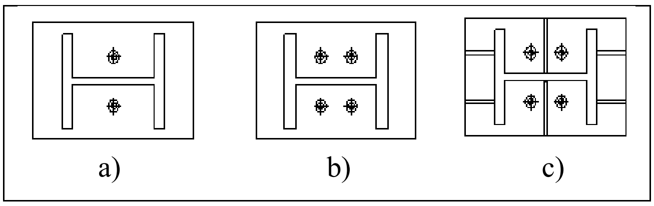

Figure 5. Hinge column base type that used in analysis

Where $N_{\mathrm{cr,FE}}$ is the finite-element critical load and $N_{\mathrm{cr,Euler}}$ is the Euler reference load. The error values were then evaluated against k/i_c to determine the maximum relative stiffness for which the hinged idealization remained sufficiently accurate.

For the nominally rigid configurations shown in Figure 6, the same procedure was applied using the Euler critical load associated with the rigid-base reference condition adopted in the original analysis. The calculated error was evaluated as a function of k/i_c. A connection was considered effectively rigid when an additional increase in base rotational stiffness produced only a small change in the calculated critical load relative to the idealized rigid reference.

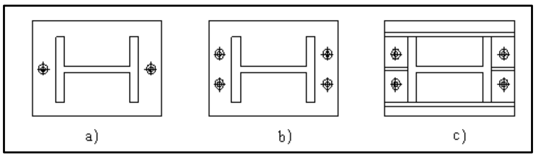

Figure 6. Rigid column base type that used in analysis

The classification thresholds were obtained from the relationship among the normalized stiffness ratio, the finite-element buckling load, and the Euler reference load. A ratio below 2 was identified as sufficiently flexible to be represented by a hinged connection. A ratio greater than 24 was identified as sufficiently stiff to be represented by a rigid connection. Ratios between these limits were classified as semi-rigid. The resulting classification criteria were

$$\frac{k}{i_c} < 2: \quad \text{hinged,} \tag{5}$$

$$2 \le \frac{k}{i_c} \le 24: \quad \text{semi-rigid,} \tag{6}$$

and

$$\frac{k}{i_c} > 24: \quad \text{rigid.} \tag{7}$$

These thresholds were derived for the geometries, material properties, contact assumptions, and loading conditions considered in the present numerical investigation. They were therefore evaluated as calculation-schema criteria rather than universal connection-strength limits.

3. Result and Discussion

The numerical analysis was conducted to evaluate the deformation characteristics, rotational stiffness, and appropriate structural idealization of exposed steel column–foundation connections. Thirteen column-base configurations were analyzed by varying the number and position of the anchor bolts and the arrangement of the stiffeners. Models 1–4 represented configurations in which the anchor bolts were positioned inside the column flanges and were conventionally treated as hinged bases, whereas Models 5–11 used anchor bolts outside the flanges and were conventionally treated as rigid bases. Models 12 and 13 combined internal and external anchor bolts, with Model 13 additionally incorporating four stiffeners. These configurations allowed the influence of the main connection components on the rotational response to be evaluated systematically. Recent experimental and numerical studies similarly demonstrate that connections conventionally designated as pinned or fixed generally possess finite and nonlinear rotational stiffness; consequently, their behavior should be evaluated through the interaction among the base plate, anchor bolts, concrete foundation, and stiffeners rather than solely from the nominal connection detail [5][6][7][8][9][10].

The finite element model consisted of an H-shaped steel column, a steel base plate, anchor bolts, nuts, stiffeners where applicable, and a concrete foundation. The adopted mesh arrangement is shown in Figure 3. Approximately 3000 elements were used for the column, 4000 elements for the concrete foundation, 2000 elements for the base plate, and approximately 500 elements for the anchor bolts, nuts, and stiffeners, resulting in approximately 9000–10,000 elements for each model. Eight-node reduced-integration solid elements, C3D8R, were used for all components. Tie constraints were assigned to the welded or fully connected interfaces, while surface-to-surface contact was used between the base plate and foundation and between the anchor bolts, nuts, and base plate. Friction coefficients of 0.40 and 0.15 were assigned to the base plate–

foundation and steel-component interfaces, respectively. The embedded-region constraint was applied between the anchor bolts and the concrete foundation. The use of three-dimensional solid elements and explicit interface contact is necessary because separation, bearing, friction, and local plate bending contribute directly to the moment–rotation response. Similar modeling approaches have recently been adopted to reproduce base-plate uplift, anchor-bolt elongation, concrete bearing, and nonlinear moment–rotation behavior [7][8][9][10][11][12][13].

Figure 7 presents the deformed shape of Model 8 under the combined horizontal and vertical loads. The deformation pattern shows that rotation initially developed through local deformation of the base plate and elongation of the tension-side anchor bolts rather than through flexural deformation of the steel column alone. Although Model 8 was initially regarded as a rigid column base because its anchor bolts were located outside the column flanges, the connection exhibited measurable rotation. This observation indicates that an exposed base cannot be treated as perfectly fixed merely because the anchor bolts are positioned outside the column profile. The deformation mechanism consists of uplift on the tension side, bearing of the plate against the concrete on the compression side, tensile elongation of the anchor bolts, and local bending of the projecting portions of the base plate. Recent studies confirm that such interactions produce a nonlinear and semi-rigid response even in connections conventionally classified as fixed [7][10][11][13].

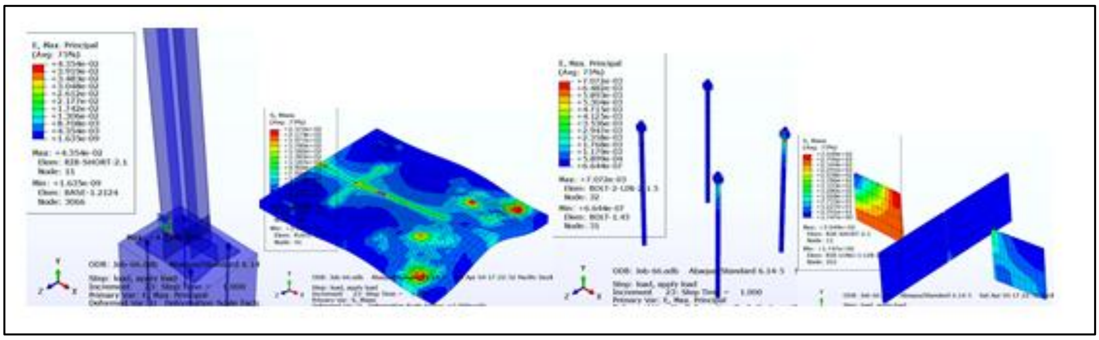

Figure 7. Deformation of the Model 8

The angular deformation of the base plate was evaluated using the vertical the vertical displacement of two monitoring points shown in Figure 4. The first point was located near the center of the base plate, while the second point was positioned at the centerline of the tension-side column flange. The base-plate rotation was calculated from the relative vertical displacement between these points according to

$$\theta = \frac{\Delta_i - \Delta_j}{y_i - y_j} \tag{8}$$

Where θ is the rotation of the column-base connection, Δ_i and Δ_j are the vertical displacements of the monitoring points, an y_i and y_j are their corresponding coordinates. This displacement-based procedure captures the local rotation at the base plate more directly than a rotation curve, the initial tangent stiffness, stiffness degradation, and the post-yield response, as emphasized in recent experimental and fin element investigations [5][6][9][12][13].

The calculated vertical displacements and rotations of Models 1–13 are summarized in Table 4. The results demonstrate substantial variation among the configurations, confirming that the rotational response depends on the arrangement of the connection components. Models 1 and 2, which used two anchor bolts inside the column flanges, developed relatively large rotations of 0.1004 and 0.120 rad, respectively. These values indicate flexible behavior but also show that the connections retained a finite capacity to resist bending moment. Model 5, which had two external anchor bolts, developed a smaller rotation of 0.0386 rad. The addition and reorientation of stiffeners reduced the rotation further, as observed in Models 6 and 7. Model 13, which combined internal and external anchor bolts with four stiffeners, exhibited considerably smaller displacement than the unstiffened configurations. These results support the interpretation that neither nominally pinned nor nominally rigid exposed bases behave as ideal boundary conditions.

Table 4. The analyze results of the Model 1~13

Model number	1	2	3	4	5	6	7	8	9	10	11	12	13
Δ_1(mm)	51.21	61.45	26.8	30.6	33.48	21.26	13.72	13.64	14.1	10.3	11.45	23.73	3.33
Δ_2(mm)	73.3	87.96	43.37	41.1	42.01	27.02	17.98	17.9	19.09	13.5	15.1	35.36	4.04
θ(rad)	0.1004	0.12	0.0753	0.0502	0.0386	0.0264	0.0194	0.0194	0.0023	0.0145	0.0165	0.0529	0.0033

The comparison between Models 1 and 5 in Figure 8 illustrates the effect of locating the anchor bolts inside or outside the column flanges. Model 1, with two internal anchor bolts, experienced larger plate deformation than Model 5, with two external anchor bolts. Locating the bolts outside the flanges increased the effective lever arm between the tension force in the anchor bolts and the compression resultant beneath the base plate. Consequently, a given bending moment could be resisted with a lower anchor-bolt tensile force, while the wider force couple reduced the overall connection rotation. This finding is consistent with recent experimental evidence showing that anchor-bolt layout strongly affects initial rotational stiffness, bending resistance, and the distribution of tensile forces among the bolts [5][11][12].

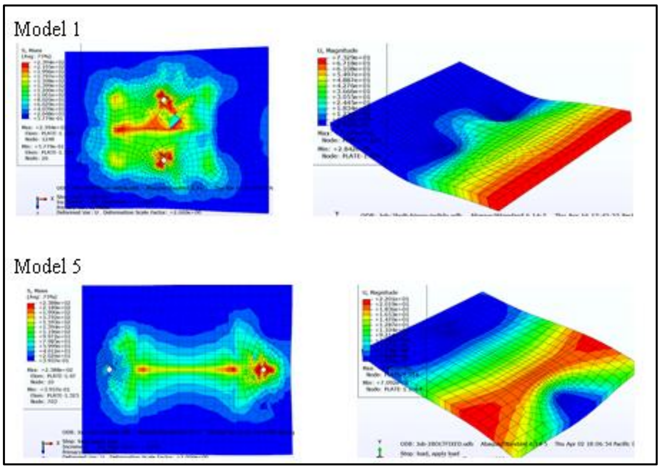

Figure 8. Stress and deformation of the base plate in Model 1, 5

The comparison between Models 1 and 2 in Figure 9 indicates that increasing the distance of the internal anchor bolts from the column center did not automatically produce lower local plate deformation. Although a larger bolt lever arm generally increases the global moment resistance, it can also increase the unsupported plate projection and alter the prying action between the column flange, base plate, and anchor bolt. The observed increase in deformation in Model 2 should therefore be interpreted as the combined effect of bolt eccentricity and local base-plate flexibility rather than as the effect of lever arm alone. The response of an anchor bolt cannot be separated from the bending behavior of the surrounding plate because the tensile force transmitted by the bolt can induce local plate curvature and secondary bending in the anchor rod. Similar component interaction and prying effects have been reported in recent nonlinear studies of stiffened and unstiffened column bases [7][11].

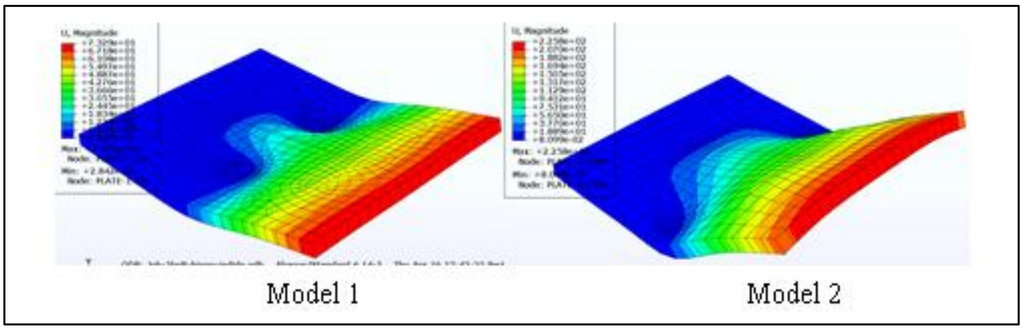

Figure 9. Deformation of the base plate in Model 1, 2

Figure 10 compares Models 8 and 9, both of which contained four external anchor bolts. The difference in the deformation pattern shows that moving the anchor bolts farther from the column affects not only the effective force couple but also the flexible length and deformation mode of the base plate. A larger bolt spacing may improve the nominal moment arm, but its benefit can be offset when the plate region between the column flange and anchor-bolt line becomes more flexible. Consequently, the anchor-bolt layout should be optimized together with the plate thickness and stiffener arrangement. Recent numerical simulations show that linearly arranged outer anchor bolts do not necessarily share the tension demand uniformly, whereas alternative layouts can improve force distribution and connection efficiency [11].

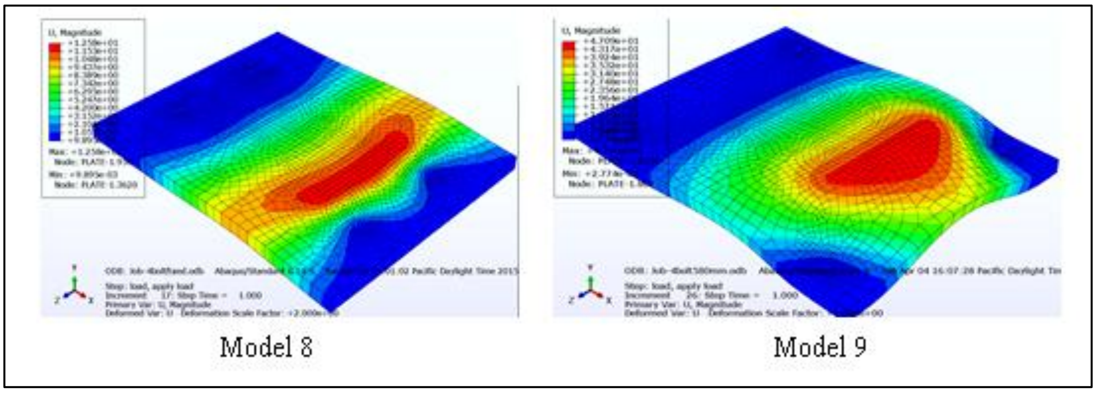

Figure 10. Deformation of the base plate in Model 8, 9

The deformation patterns of Models 4, 8, and 12 are compared in Figure 11. Each model contained four anchor bolts, but their positions relative to the column flanges differed. Model 4 used internal bolts, Model 8 used external bolts, and Model 12 combined internal and external bolts. Model 8 produced the smallest deformation among these three configurations, while Model 12 produced the largest. This result demonstrates that increasing the total number of bolts does not by itself guarantee a proportional increase in rotational stiffness. The contribution of each anchor bolt depends on its distance from the compression resultant, the flexibility of the base plate around the bolt line, and the compatibility of deformation among the internal and external bolts. The combined layout in Model 12 may have resulted in nonuniform tensile-force distribution, with some bolts attracting substantially more force than others. Similar nonuniformity has been observed in recent parametric investigations, particularly when several anchor bolts are arranged in linear rows [11].

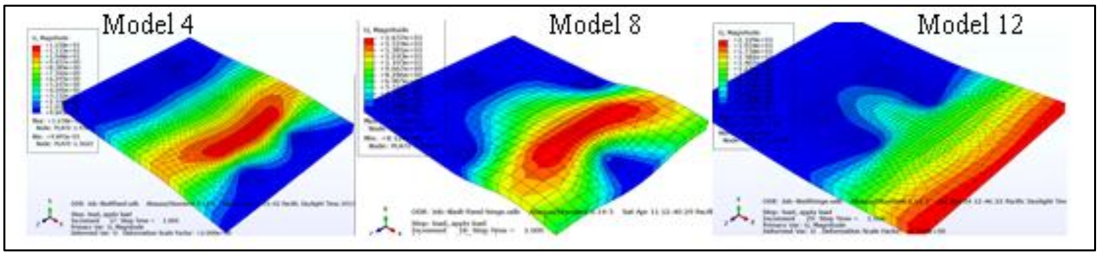

Figure 11. Deformation of the base plate in Model 4, 8, 12

The effect of stiffening is evident from the comparison of Models 1 and 3 in Figure 12. Model 3 was obtained by adding stiffeners to the configuration of Model 1, and its rotation decreased from 0.1004 to 0.0753 rad, as reported in Table 4. The stiffeners reduced local bending of the base plate by transferring part of the flange force more directly into the plate and anchor-bolt region. However, the reduced plate deformation may increase the tensile demand on the anchor bolts and may shift the governing failure mode from plate yielding to anchor-bolt yielding or fracture. Therefore, stiffeners should not be evaluated solely from the reduction in rotation; their effects on connection strength, ductility, weld demand, and bolt-force distribution must also be considered. Recent research shows that stiffeners generally increase stiffness and resistance but may reduce rotational ductility and generate additional stress concentrations near welded regions [7][11].

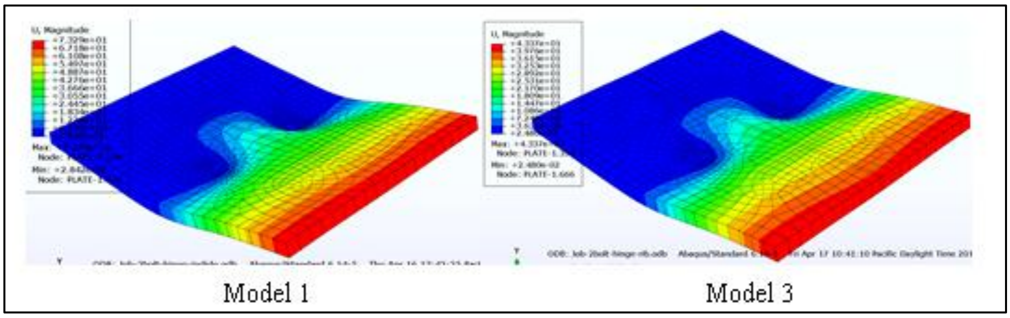

Figure 12. Deformation of the base plate in Model 1, 3

The orientation of the stiffeners also influenced the response, as demonstrated by Models 5–7 in Figure 13. Model 5 was unstiffened, whereas Models 6 and 7 incorporated stiffeners in different directions. The stiffeners aligned more effectively with the direction of bending produced a greater reduction in base-plate deformation than those oriented perpendicular to the principal moment. This behavior is mechanically reasonable because a stiffener aligned with the flange-force path increases the out-of-plane bending rigidity of the plate in the region where tensile uplift and compression bearing are concentrated. The results therefore indicate that stiffener effectiveness depends on orientation and continuity with the column flange, not merely on the presence of additional steel. The finding is consistent with recent studies reporting that stiffener geometry and orientation influence stress transfer, local anchor-rod bending, connection stiffness, and the governing failure mode [7][11].

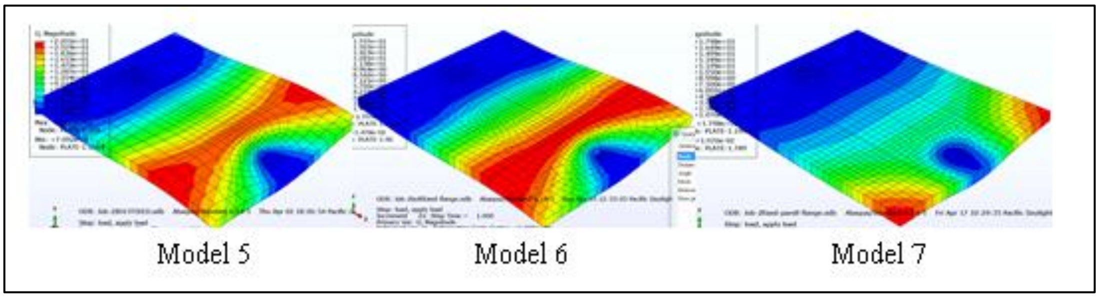

Figure 13. Deformation of the base plate in Model 5~7

Collectively, Figures 8-13 and Table 4 show that the rotational response is governed by an interacting system rather than by a single geometric parameter. Increasing the number of active tension-side anchor bolts generally improves stiffness, but the improvement depends on the force distribution between the bolts. Moving the bolts outward increases the nominal lever arm, although excessive plate projection may increase local plate bending. Adding stiffeners reduces base-plate deformation, but may lower connection ductility or transfer greater demand to the anchor bolts and welds. These interactions explain why a connection with internal bolts can resist a nonzero moment and why a connection with external bolts cannot be assumed to be perfectly rigid. Experimental studies on internal anchor-bolt connections have likewise shown measurable stiffness and moment resistance in bases conventionally described as pinned [5], while recent studies of nominally pinned gravity bases found rotational stiffness substantially greater than the idealized design value [8].

Based on the observed deformation mechanism, the rotational stiffness of the exposed column base was related to the axial stiffness of the tension-side anchor bolts and the effective distance between the tension and compression resultants. Equation (2) incorporates the area and elastic modulus of the tensioned anchor bolts, the number of active bolts, the embedment or deformable length of the bolts, the distance from the column-base center to the tension-side bolts, the distance to the compression resultant, and a reduction factor representing base-plate deformation. The reduction factor distinguishes stiffened and unstiffened configurations and accounts approximately for the fact that part of the total rotation originates from plate bending rather than anchor-bolt elongation. The physical basis of the equation is consistent with component-based interpretations in which the connection rotation is obtained from the deformation compatibility of the tension and compression components. However, because the compression-zone position and plate flexibility may vary with load, Equation (2) should be treated as an equivalent stiffness expression for the investigated range rather than as a universal constant. Recent research similarly shows that rotational stiffness varies with the load level, axial force, base-plate uplift, bolt diameter, plate thickness, and contact condition [8][9][10][13].

The proposed connection classification was evaluated through buckling analyses of steel columns with different section dimensions and lengths. The analyzed column properties are presented in Table 1. Because the structural consequence of a given base stiffness depends on the flexural stiffness and length of the supported column, the column base cannot be classified using the absolute rotational stiffness alone. The relevant nondimensional parameter is the ratio between the connection rotational stiffness, k, and the column stiffness per unit length, ic = EI/L. This normalized ratio indicates whether the connection rotation is large or small relative to the flexural deformation of the column. The use of a relative stiffness measure is also consistent with recent frame-level studies in which the base stiffness is normalized by the column flexural rigidity to represent the transition between pinned, semi-rigid, and fixed behavior [8][14].

Figure 5 shows the column-base configurations used to evaluate nominally hinged behavior, while the corresponding buckling results are presented in Table 2. The table compares the critical loads obtained from the finite element models with the Euler critical loads calculated for an ideal hinged condition. For the type-a configurations, the normalized stiffness ratio k/ic generally ranged from approximately 0.90 to 2.69, and the difference from the ideal hinged Euler load was generally limited to approximately 1.82–9.42%. When k/ic approached approximately 2, the difference was generally around 6.5% or less, whereas a ratio of approximately 2.8 corresponded to an error close to 10% in the selected comparison cases. In contrast, the type-b and type-c bases had larger stiffness ratios and produced progressively greater deviations from the ideal hinged solution. These results indicate that treating the base as an ideal hinge is reasonable only when its rotational stiffness is sufficiently small in relation to *EI/L*.

On the basis of Table 2, the column–foundation connection may be classified as effectively hinged when *k/ic* < 2. This limit does not imply zero rotational stiffness. Instead, it indicates that the finite base stiffness produces only a relatively small difference in the column buckling response compared with the ideal hinged model. This distinction is important because a physically detailed exposed base may resist moment while still being represented as a hinge for a specified global-analysis purpose. Recent investigations support this interpretation by showing that nominally pinned bases possess nonzero stiffness and may attract considerable moment even when their global response remains closer to a pinned than a fixed idealization [5][8][9].

Figure 6 presents the column-base configurations used to assess nominally rigid behavior, and the corresponding results are listed in Table 4. The normalized ratio (k/i_c) for the type-c configurations ranged from approximately 11.79 to 35.24. Cases with ratios greater than approximately 24 generally showed small differences from the Euler critical load associated with the ideal fixed-base condition, whereas the difference increased as the ratio decreased below this level. The type-b and type-a configurations, which had lower rotational stiffness, showed substantial discrepancies and could not be represented reliably as fully fixed bases. These results demonstrate that a connection must be considerably stiffer than the column flexural stiffness per unit length before the ideal fixed assumption becomes appropriate.

Accordingly, a value of k/ic > 24 is proposed as the threshold for an effectively rigid column–foundation connection. Values between 2 and 24 represent semi-rigid behavior because neither the ideal pinned nor the ideal fixed model provides a sufficiently accurate description of the calculated buckling response. The proposed classification is therefore

$$\frac{k}{i_c} < 2 \text{ hinged connection,} \tag{9}$$

$$2 \leq \frac{k}{i_c} \leq 24 : \text{semi-rigid connection,} \tag{10}$$

$$\frac{k}{i_c} > 24 : \text{rigid connection.} \tag{11}$$

This classification provides a rational link between local connection behavior and global column response. It also avoids defining the boundary condition solely from the anchor-bolt location or the presence of stiffeners. The results show that Models 1 and 2, despite being conventionally designated as hinged, developed finite moment resistance, while several configurations conventionally designated as rigid showed appreciable base-plate deformation. Therefore, Models 3–12 are more appropriately treated as semi-rigid for the investigated geometry and loading conditions unless their normalized stiffness satisfies one of the limiting criteria.

The proposed limits should nevertheless be interpreted within the scope of the present analysis. The numerical program considered a specific column section, base-plate dimension, concrete strength, anchor-bolt diameter and embedment, contact model, and loading direction for the deformation study. The classification was subsequently examined using the column sections and lengths in Table 1, but no physical experimental validation of the thirteen connection models was presented. The models also used monotonic loading, whereas repeated or cyclic loading can produce opening and closing of the base plate, pinching, anchor-bolt yielding, concrete damage, stiffness degradation, and residual deformation. Recent cyclic and biaxial studies indicate that connection stiffness and failure mechanisms can change significantly with the loading direction, axial-force level, and number and layout of the anchor bolts [5][6][12][13]. In particular, connections with eight anchor bolts have been observed to provide greater rotational stiffness than otherwise comparable four-bolt arrangements under combined axial and biaxial loading [12].

The analysis also indicates that axial force should be incorporated explicitly when the proposed stiffness equation and classification limits are validated. Axial compression may enhance contact between the base plate and concrete and increase rotational stiffness before uplift, whereas axial tension can separate the plate from its support and substantially reduce stiffness. Recent full-scale tests and calibrated finite element models found that replacing axial compression with tension can cause a very large reduction in rotational stiffness, particularly for thin plates and small-diameter anchor bolts [9][10]. Similarly, recent investigations of gravity column bases found that the applied compression ratio had a pronounced influence on both moment resistance and rotational stiffness [8]. From a structural-design perspective, the semi-rigid range is particularly important because neglecting finite base stiffness can alter the predicted effective length, buckling load, internal-force distribution, lateral displacement, and frame period. A pinned idealization may underestimate the moment transferred to the foundation and the bottom of the column, whereas an ideal fixed assumption may overestimate the lateral stiffness and underestimate drift. Recent frame-level nonlinear analyses demonstrate that increasing base rotational stiffness can reduce fundamental periods and interstory drift but may increase floor accelerations and redistribute yielding within the structure [14]. Therefore, the selection of the analysis schema should be based on the calculated connection stiffness and the stiffness of the connected column rather than on a nominal detailing category alone.

Overall, the results establish that exposed steel column bases form a continuum between ideal hinge and ideal fixity. Anchor-bolt number and position, bolt axial stiffness, base-plate flexibility, stiffener orientation, and the effective compression-zone location jointly control the connection rotation. The proposed rotational-stiffness equation provides a simplified means of representing these effects, while the normalized ratio (k / (EI/L)) links the local connection response to the global behavior of the column. Within the investigated parameter range, ratios below 2 may be represented as hinged, ratios above 24 may be represented as rigid, and intermediate values should be modeled as semi-rigid. Further experimental validation under monotonic, cyclic, weak-axis, and biaxial loading is required before the thresholds are applied beyond the geometric and material conditions considered in this study.

4. Conclusion

This study investigated the deformation behavior, rotational stiffness, and structural classification of exposed steel column–foundation connections using three-dimensional finite-element analysis. Thirteen column-base configurations were examined by varying the number and position of the anchor bolts and the arrangement of the stiffeners. The results demonstrate that exposed column bases do not behave as perfect hinges or perfectly fixed supports. Connections nominally detailed as hinged can transfer bending moment, while connections nominally detailed as rigid can undergo measurable rotation because of base- plate bending, anchor-bolt elongation, contact separation, and concrete bearing.

The deformation analysis showed that anchor-bolt number, anchor-bolt position, base-plate flexibility, and stiffener arrangement jointly govern connection behavior. Increasing the number of effective tension-side anchor bolts generally reduced deformation, although the improvement depended on the distribution of bolt forces and the flexibility of the surrounding plate. Moving the anchor bolts farther from the column center increased the nominal moment arm but could also increase the unsupported plate projection and local plate bending. Consequently, a larger bolt spacing did not necessarily produce a stiffer connection.

The use of stiffeners reduced the local deformation of the base plate. Stiffeners aligned with the principal bending and column-flange force-transfer direction were more effective than stiffeners oriented perpendicular to that direction. Nevertheless, increasing the plate rigidity can transfer greater forces to the anchor bolts and welds. Stiffener design should therefore consider not only the reduction in rotation but also bolt demand, weld stress, connection ductility, and the governing failure mechanism.

The rotational stiffness of the exposed column base was represented using the axial stiffness of the tension-side anchor bolts, the number and arrangement of active bolts, the effective tension–compression lever arm, and a reduction factor accounting for base-plate deformation. This formulation provides a mechanical link between the local deformation of the connection components and the overall moment– rotation response. However, the reduction factor and effective component dimensions require further calibration against experimental results.

The buckling analysis confirmed that the absolute rotational stiffness of a column base is insufficient for selecting an appropriate calculation schema. The structural effect of the connection depends on its stiffness relative to the flexural stiffness and length of the connected column. The ratio , with , was therefore used as the governing classification parameter.

Within the parameter range investigated, a column–foundation connection may be represented as hinged when $k/ic < 2$. A connection may be represented as rigid when $k/ic > 24$. Connections for which $2 \leq k/ic > 24$ should be modeled as semi-rigid. These limits provide a rational basis for selecting the calculation schema because they relate local connection stiffness directly to global column behavior.

The proposed thresholds remain subject to the assumptions adopted in the finite-element models, including the selected column and plate dimensions, anchor-bolt diameter and embedment, concrete properties, contact coefficients, loading direction, and monotonic load condition. Further research should include full-scale experimental validation, mesh-sensitivity assessment, variation of axial load, cyclic loading, weak-axis and biaxial bending, concrete damage, grout behavior, and alternative anchor-bolt layouts. Such investigations are necessary before the proposed classification limits are generalized to a broader range of exposed steel column-base connections.

5. Acknowledgements

The authors have no specific acknowledgements to declare.

6. Conflict of Interest

The authors declare that they have no known financial or personal conflicts of interest that could have influenced the research presented in this article.

References

[1] J. C. Ermopoulos and G. N. Stamatopoulos, "Mathematical modelling of column base plate connections," J. Constr. Steel Res., vol. 36, no. 2, pp. 79–100, 1996, doi: 10.1016/0143-974X(95)00011-J.

[2] J.-P. Jaspart and D. Vandegans, "Application of the component method to column bases," J. Constr. Steel Res., vol. 48, nos. 2–3, pp. 89–106, 1998, doi: 10.1016/S0143-974X(98)90196-1.

[3] K. K. Hon and R. E. Melchers, "Experimental behavior of steel column bases," J. Constr. Steel Res., vol. 9, no. 1, pp. 35–50, 1988, doi: 10.1016/0143-974X(88)90055-7.

[4] European Committee for Standardization, Eurocode 3: Design of Steel Structures—Part 1-1: General Rules and Rules for Buildings, EN 1993-1-1:2005. Brussels, Belgium: CEN, 2005.

[5] J. Pan, R. Huang, J. Xu, P. Wang, Z. Wang, and J. Chen, "Behavior of exposed column-base connections with four internal anchor bolts under seismic loading," Structures, vol. 34, pp. 105–119, 2021, doi: 10.1016/j.istruc.2021.07.016.

[6] D. Zhao, Y. Shan, P. Wang, and J. Xu, "Seismic performance analysis of exposed column-base connections along minor axis," J. Constr. Steel Res., vol. 197, Art. no. 107430, 2022, doi: 10.1016/j.jcsr.2022.107430.

[7] B. C. Mehdi, N. Boumechra, A. Missoum, and A. Bouchair, "Connection of a steel column base plate: Mechanical behavior and stiffening effects," Civil Eng. J., vol. 8, no. 9, pp. 1764–1786, 2022, doi: 10.28991/CEJ-2022-08-09-02.

[8] J. C. W. He, G. C. Clifton, S. Ramhormozian, and L. S. Hogan, "Numerical and analytical study of pinned column base plate connections," J. Constr. Steel Res., vol. 204, Art. no. 107846, 2023, doi: 10.1016/j.jcsr.2023.107846.

[9] M. T. Nawar, E. Matar, A. El-Zohairy, A. Alaaser, and H. Maaly, "Experimental and FE analysis of the behavior of steel column base connections under tension and bending moment," Structures, vol. 62, Art. no. 106164, 2024, doi: 10.1016/j.istruc.2024.106164.

[10] M. T. Nawar, A. El-Zohairy, A. G. Alaaser, and O. Hamdy, "Finite element analysis and optimization of the rotational stiffness of semi-rigid base connection under simultaneous moment and tension," Buildings, vol. 14, no. 7, Art. no. 2166, 2024, doi: 10.3390/buildings14072166.

[11] R. Khani, M. D'Aniello, R. Tartaglia, and Y. Hosseinzadeh, "Parametric finite element simulations of different configurations of partial-strength exposed column base plate connections," Buildings, vol. 15, no. 13, Art. no. 2255, 2025, doi: 10.3390/buildings15132255.

[12] K. Roller, A. H. M. M. Billah, M. A. B. Kabir, A. Elshaer, and A. Iqbal, "Experimental investigation of exposed column base plate connections subjected to combined axial load and biaxial bending," Eng. Struct., vol. 342, Art. no. 120890, 2025, doi: 10.1016/j.engstruct.2025.120890.

[13] S. Jiang and A. H. M. M. Billah, "Finite element simulation and parametric study of exposed column base plate connections under axial compression and bi-directional lateral loading," J. Build. Eng., vol. 111, Art. no. 113188, 2025, doi: 10.1016/j.jobe.2025.113188.

[14] S. Jiang and A. H. M. M. Billah, "Effect of base connection rotational stiffness on seismic performance of steel moment resisting frames," J. Build. Eng., vol. 117, Art. no. 114936, 2026, doi: 10.1016/j.jobe.2025.114936.